Design Considerations for the Brushless Doubly Fed (Induction) Machine

R. A. McMahon*, M.E. Mathekga†, X. Wang‡, M.R. Tatlow*
* Electrical Engineering Division, University of Cambridge, 9 JJ Thomson Avenue, Cambridge, CB3 0FA, UK
{ram1,mrt39}@cam.ac.uk
‡ GE Power Conversion, Boughton Road, Rugby, CV21 1BU, UK
xiaoyan.wang@ge.com
† CSIR Modelling and Digital Science Unit. Meiring Naude Road, Pretoria, 0184, South Africa
dmathekga@csir.co.za

Abstract

A design procedure for the Brushless Doubly Fed machine is based on equations derived from a simplified equivalent circuit. The method allows the many variables in the design of this machine to be handled in straightforward way. Relationships are given for the division of slot area between the two stator windings and for the design of the magnetic circuit. The design method is applied to a frame size 180 machine. In particular, calculated values for flux densities in the machine have been verified by time stepping finite element analysis for actual operating conditions. The approach outlined can also be used as part of a design optimization routine.

List of Symbols

p, p_1, p_2	Number of pole pairs: general, and for stator windings 1,2
$n_r, n_{r_{opt}}$	Rotor turns ratio: general and optimal
f, f_1, f_2	Frequency: general, and for excitations of stator windings 1,2
N_r, N_n	Rotor speed and BDFM natural speed
N_i	Number of turns of winding i
P_1, P_2	Real powers of stator windings 1,2
P_{c_1}, P_{c_2}, P_c	Real powers of stator winding 1,2 and total computed from BDFM core model
S_c	BDFM rating from core model
d	Airgap diameter
g	Effective airgap length
l	Effective stack length
$\bar{J}_c, \bar{J}_1, \bar{J}_2$	Electrical loading of core model, stator 1,2
$\bar{J}_{r_{p1}}, \bar{J}_{r_{p2}}$	Electrical loading of rotor mmf harmonics corresponding to the $2p_{1,2}$ fields
J_s	Conductor current density
c_p	Slot fill factor
B, B_1, B_2	RMS value of airgap magnetic field density: general, and that generated by stator windings 1,2
N, N_1, N_2	Number of turns: general, and for stator windings 1,2
k_{w1}, k_{w2}, k_w	Winding factor: general, and for stator windings 1,2
α	Proportion of stator slot area assigned to stator winding 1
δ	Load angle
ϕ	Phase angle between power winding voltage and current phasors
$\bar{B}$	Magnetic loading
B_{sum}, B_{quad}	Sum and quadrature sum of stator windings 1,2 flux densities
B_t, B_c	Peak teeth and core back magnetic flux densities
$B_{t,s}, B_{c,s}$	Peak tooth and core back magnetic flux densities for stator
$B_{t,r}, B_{c,r}$	Peak tooth and core back magnetic flux densities for rotor
V, V_1, V_2	Voltage: general, and applied to stator winding 1,2
w_t	Tooth width
y_c	Core back width

I. Introduction

The brushless doubly fed machine (BDFM) is attractive as a variable speed generator or drive as only a fractional converter is required. Using the machine as a generator in wind turbines was first proposed by Wallace et al. [1] and subsequent interest has been primarily focused on this application [2], [3]. The absence of brushgear offers the advantage of lower maintenance compared to conventional slip-ring induction generator and recent work by Arabian et al. [4] has shown that use of the BDFM should lead to a system with higher reliability. The machine has also been considered as a drive [5].

The BDFM has its origins in the self-cascaded machine [6] and it has two stator windings of different pole numbers and a specially designed rotor winding, which couples to both stator windings all wound on a common stator and rotor core. The modern BDFM, as developed at Oregon State University [7], has two electrically separate stator windings and is designed to operate in a synchronous mode, as is usual in slip-ring induction generators. It is common practice to refer to a BDFM by the pole numbers of the two windings, for example a 2-pole/6-pole BDFM, or 2/6 BDFM for short.

Various BDFMs have been reported in the literature. Some machines have been designed specifically for wind power applications [2], [8] whereas other have been primarily research tools, for example [9], [10]. Whilst attention has been given to some aspects of BDFM design [11]–[13], there remains a need for a deeper understanding of the design of a BDFM, especially as there are more machine variables compared to conventional induction machines.

This paper develops a design procedure based on analytical relationships, initially derived from a simplified form of the equivalent circuit model proposed by Roberts et al. [10]. Adjustments to the design to take into account magnetizing currents and actual operating conditions including speed range and power factor are then made using the approach reported by the authors in [12], again using the equivalent circuit approach. Time-stepping finite element analysis (TSFEA) is used to verify the magnetic design formulae. The design process is illustrated with results from a frame size 180 BDFM.

II. BDFM Operation

The BDFM is connected as shown in Figure 1 for controlled variable speed operation in the synchronous mode. Stator windings 1 and 2 are functionally known as the power (PW) and control (CW) windings. In the synchronous mode the shaft speed, independent of torque, is given by:

$$N_r = \frac{60\,(f_1 + f_2)}{(p_1 \pm p_2)} \tag{1}$$

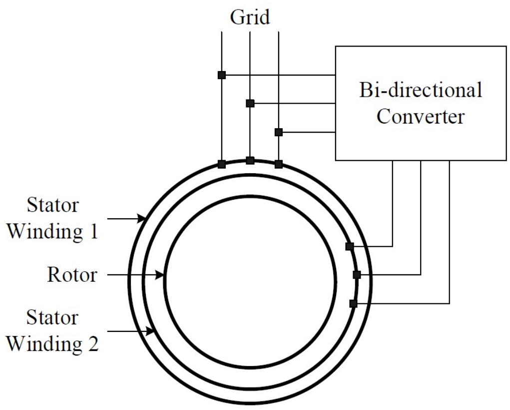

Fig. 1: The usual connection of the BDFM for the synchronous mode of operation

The speed when the frequency of the control windings (f_2) is equal to zero, i.e. the control winding supplied with DC, is called the natural speed (N_n) and is analogous to the synchronous speed of the induction machine. The speed of the BDFM above and below N_n is obtained by different control winding excitation sequences, equivalent to supplying positive and negative frequencies. Previous analysis [14] shows that induction torque components are also present in synchronous mode operation but these will be a relatively small in a well-designed machine.

III. Choice of pole numbers

The choice of stator and rotor winding pole-pair numbers to give a desired natural speed is the first step in the design process. All reported BDFMs to date have been of the $p_1 + p_2$, or cumulative type, but the $p_1 - p_2$ form or differential type of BDFM is also possible, as noted by Williamson et al. [15]. However, as pointed out by Broadway and Burbridge [6], the differential type machine has significant drawbacks so only the the cumulative type is considered in this paper. It is important to note that the torque capability of a BDFM collapses as the speed of the machine approaches the synchronous speed of the p_1 field, i.e. of the stator power winding. However, to gain most advantage in terms of reduced converter rating, the range of operating speeds is likely to be limited. For example, in wind power applications, it may be the natural speed $\pm 30\%$ so the loss of torque does not need to be considered.

There should not be any direct coupling between the two stator windings. For fully pitched windings, choosing pole-pair numbers according to the following rules allows this to be achieved, subject to the appropriate connection of coils. On the basis that p_1 is smaller than p_2, the rules are:

(i) p_1 is even and p_2 is odd (or vice versa), or

(ii) p_1 and p_2 are even as long as p_2/p_1 is not odd (p_2/p_1 does not need to be an integer).

Choosing pole-pair combinations that differ by one leads to unbalanced magnet pull. A further class of BDFMs is possible in which cross-coupling between stator windings does occur but is zero sequence. Machines with $p_1/p_2 = kq$, where q is the phase number of the supply and k is an integer, fall into this category. The obvious example, identified by Creedy [16], is the $2/6$ BDFM; this also is the cumulative type BDFM with the highest natural speed.

In practice, a designer is likely to use short pitched stator windings to reduce space harmonics; this means that direct coupling can become possible. Care is therefore needed to ensure that the coils are connected in such a way that the emfs from cross-coupling are cancelled. Similarly, combinations of pole-pairs disallowed by the above rules can be used if techniques such as fractional slot pitching are employed.

In cases where there is more than one permissible combination of pole-pair numbers, the designer must judge between output torque, speed, and magnetization considerations to determine the most appropriate combination. A further factor is vibration [17]. The authors have always used the lower pole number winding as the power winding. This has two obvious advantages, firstly the synchronous speed of the power winding at which the torque collapses is further away from the machine's natural speed, permitting a wider operating speed range. In addition, the reactive power demanded from the mains is reduced. However, the rotor frequency is higher in this configuration and this has been cited as a reason for using the higher pole number winding as the power winding [18].

IV. Machine Rating

Basic design relationships can be derived from the simplified per-phase equivalent circuit of the BDFM shown in Figure 2. The main advantage of this form of equivalent circuit, in which the stator leakage inductances are not explicitly shown, is that all quantities can be determined from terminal measurements [10]. It is assumed that the rotor parameter values defined in Table I , are sensibly independent of rotor speed. Values are shown referred to the power winding on the left and iron losses are neglected. The prediction of iron loss is not straightforward due to the complex distribution of the magnetic field in the machine, which requires careful evaluation. There has been research into predicting core losses most notably by Ferreira et. al [19], but to date no satisfactory solution has been found.

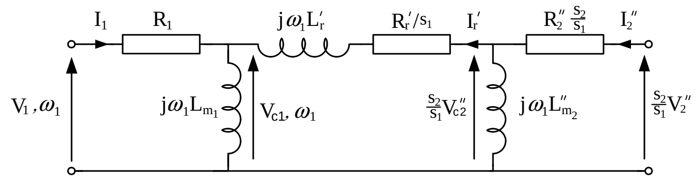

Fig. 2: A simplified referred per-phase equivalent circuit model of the BDFM

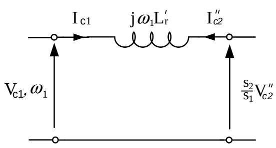

Fig. 3: BDFM core model

To simplify the analysis further, the equivalent circuit model is reduced to the form shown in Figure 3, where the magnetising inductances together with stator and rotor resistances have been omitted. The rotor leakage reactance is retained as it is usually the dominant series component in a practical BDFM.

An equation for the total output power of the BDFM was derived using this model in [14] and is given by:

$$P_c = \frac{\pi^2}{\sqrt{2}} \left(\frac{d}{2}\right)^2 l\omega_r \bar{B} \bar{J}_c \left(\frac{p_1 + p_2}{p_1 \left(1 + \frac{1}{n_r}\right) \sqrt{1 + \left(\frac{n_r p_2 \cos\phi}{p_1 \cos(\phi + \delta)}\right)^2}} \right) \cos\phi \tag{2}$$

TABLE I: Equivalent circuit parameters

Parameter	Description
R_1	Stator 1 resistance
R_2''	Stator 2 resistance, referred
R_r'	Rotor resistance, referred
L_{m_1}	Stator 1 magnetizing inductance
L_{m_1}''	Stator 2 magnetizing inductance, referred to stator 1
L_r'	Rotor inductance, referred to stator 1
s_1	Slip of stator 1 field
s_2	Slip of statir 2 field
n	Turns ratio

There is not an analytical expression for the magnetic loading ($\bar{B}$), but a proxy based on the quadrature sum of B_1 and B_2 was given in [14] as:

$$\bar{B} = \frac{2\sqrt{2}}{\pi} B_{quad} \tag{3}$$

With B_{quad} being:

$$B_{quad} = \sqrt{B_1^2 + B_2^2} \tag{4}$$

Experience has shown that using B_{quad} gives an underestimate of the actual peak flux densities in the magnetic circuit, leading to the risk of excessive saturation in the teeth or back iron. An alternative approach is to use a $\bar{B}$ value based on the sum of B_1 and B_2.

$$B_{sum} = B_1 + B_2 \tag{5}$$

Such that

$$\bar{B} = \frac{2\sqrt{2}}{\pi} B_{sum} \tag{6}$$

This gives an output formulation, derived in Appendix B, by considering the power converted in the two electromagnetic couplings between the stators and rotor:

$$P_c = \frac{\pi^2}{\sqrt{2}} \left(\frac{d}{2}\right)^2 l \omega_r \bar{B} \bar{J}_c \left(\frac{p_1 + p_2 \left(\frac{\cos\phi}{\cos(\phi+\delta)}\right)}{p_1 \left(1 + \frac{1}{n_r}\right) \left(1 + \frac{p_2 n_r}{p_1} \frac{\cos\phi}{\cos(\phi+\delta)}\right)} \right) \tag{7}$$

Using Equation (48) instead of Equation (2) leads to an unduly conservative design in the form of a larger machine for a given rating. To compensate, a higher value of $\bar{B}$ compared to that found in a standard induction machine can be used [20].

Using equation (48) with the assumptions of near unity power factor and small load angle operation, the turns ratio for maximum output power is:

$$n_{r_{opt}} = \left(\frac{p_1}{p_2}\right)^{1/2} \tag{8}$$

This is in contrast to the result obtained from equation (2), where the optimum turns ration is:

$$n_{r_{opt}} = \left(\frac{p_1}{p_2}\right)^{2/3} \tag{9}$$

The actual values of $n_{r_{opt}}$ are 0.71 and 0.63 for a $4/8$ BDFM from equations (8) and (9) respectively.

The output from equation (2) or (48), together with the optimum turns ratio, $n_{r_{opt}}$, is the starting point for the design of the BDFM, once the choice of pole numbers has been decided. The output power contributions from both windings is related by:

$$P_{c2} = \left(\frac{N_r}{N_n} - 1\right) P_{c1} \tag{10}$$

V. Stator winding design

Although the rotor is the special feature of a BDFM, it is convenient to consider the stator first. In principle, choosing pole-pair numbers for the two stator windings as outlined in section IV avoids unwanted cross-coupling. To illustrate the importance of connecting the coils of the windings correctly, consider a 4/8-BDFM. The 8-pole field never couples a fully pitched 4-pole coil but a fully-pitched 8-pole coil can respond to a 4-pole field. The elimination of cross-coupling therefore relies on the series connection of coils to cancel the emfs arising from the 4-pole field. Incorrect connection of the 8-pole coils could lead to direct coupling with the 4-pole field and induce a large voltage in the coil group which would lead to severe circulating currents. As mentioned earlier, short pitching must also be taken into account.

The number of stator slots appropriate to the frame size must be chosen to accommodate the two stator windings and division of the stator slot area between the two windings is a key step. It is assumed that the rotor winding can match the electric loading of the stator windings, n_r is known, and that the stator windings are equally loaded. The electric loading, is therefore given by: [14]

$$\bar{J}_c = \frac{6}{\pi d} N_1 I_{c1} k_{w1} \left(1 + \frac{1}{n_r}\right) \tag{11}$$

The contributions of stator windings 1 and 2 to $\bar{J}$ are in the ratio of $1 : 1/n_r$. Therefore,

$$\bar{J}_1 = \frac{\bar{J}}{1 + 1/n_r} \tag{12}$$

$$\bar{J}_2 = \frac{\bar{J}}{1 + n_r} \tag{13}$$

The fractions of the stator slot area allocated to the power winding, α, and control winding $(1 - \alpha)$ are given by:

$$\alpha = \frac{1}{1 + 1/n_r} \tag{14}$$

$$1 - \alpha = \frac{1}{1 + n_r} \tag{15}$$

This assumes that the current densities for the conductors and slot fill factors of both stator windings are equal. It is shown in Appendix A that dividing the slot area in this manner minimizes copper losses. In practice the slot area split needs to be adjusted to reflect achievable values of n_r, machine construction constraints and operating conditions.

The flux densities of the p_1 and p_2 air gap fields, B_1 and B_2, are related according to: [14]

$$\frac{B_2}{B_1} = \frac{n_r \cos\phi}{\cos(\phi + \delta)} \frac{p_2}{p_1} \tag{16}$$

Initial estimates of B_1 and B_2, can be computed by taking $\cos(\phi) = \cos(\phi + \delta)$ to be unity, yielding:

$$\frac{B_2}{B_1} = n_r \frac{p_2}{p_1} \tag{17}$$

The flux densities of B_1 and B_2 can then be calculated either by using B_{quad} given by equation (4) or the sum relationship given by equation (5). The details of the windings are determined knowing the intended rated voltage of the power winding, the voltage available from the converter and the desired speed deviation from natural speed which sets the converter frequency range. The number of turns (N_i) of winding i is given by:

$$N_i = \frac{p_i V_i}{2\pi f_i l d k_{w_i} B_i} \tag{18}$$

where B_i is equal to B_1 or B_2 for $i = 1$ or 2 respectively. Knowing the number of turns and the fill factor, conductor sizes can be chosen. Then, using an acceptable value of current density, current ratings can be calculated. It is recognized that the acceptable conductor current density will need to conform to limits determined by the size of the BDFM and its particular cooling arrangements and this will affect the overall electric loading of the machine. Work on the thermal modelling of the BDFM [21] shows that the two stator windings in the same stator slots are thermally closely coupled so an overall loss figure is appropriate for thermal calculations for small imbalances between the two windings. The resistance (R) of a stator coil of N turns is given by:

$$R = \frac{2\rho c N}{(\alpha d_w + l)\, A} \tag{19}$$

where ρ is the resistivity, A is the conductor cross-sectional area, d_w is the winding diameter, l is the effective stack length, α is the arc length of the end winding and c is the end winding length correction factor, slightly greater than 1.

VI. Magnetic Design

The maximum flux densities in the teeth and core back, i.e. $\hat{B}_t$ and $\hat{B}_c$, must be chosen according to some criterion e.g. to avoid saturation in the core or to minimize core losses. The tooth width, w_t, core back radial depth, y_c, and slot depth, y_s, for both the rotor and the stator laminations can then be computed using the following equations:

$$w_t = \frac{\sqrt{2}\pi d}{n_s \hat{B}_t} (B_1 + B_2) \tag{20}$$

$$y_c = \frac{\sqrt{2} d}{2\hat{B}_c} \left(\frac{B_1}{p_1} + \frac{B_2}{p_2} \right) \tag{21}$$

$$y_s = \frac{\bar{J}_c}{J_s c_p \left(1 - \frac{\bar{B}\pi}{2\hat{B}_t} \right)} \tag{22}$$

n_s is the number of rotor or stator teeth. $\bar{J}_c$ is the specific electrical loading, J_s is the conductor current density and c_p is the slot fill factor given by the machine manufacturer. Equation (21) for the core back radial depth shows the greater contribution of the lower pole number field. The airgap diameter for a given frame size can then be established using the core back and slot dimensions needed to accommodate the windings.

VII. Rotor Design

A. General principles

The rotor must couple the p_1 and p_2 fields, as discussed in section I, and should ideally have a turns ratio close to that given by equation (8). The electric loading and magnetic field density levels must be consistent with those of the stator. To achieve the same magnetic field density as the stator, the magnetic circuit must be sized according to the equations in section VI. The rotor slots must have enough conductor area for the stator electrical loading to be balanced, with an acceptable current density in the rotor conductors. The number of rotor slots is determined by the type of winding and the need to minimize unwanted cogging torques arising from interaction with the stator slotting. Finally, the rotor slot shape has to be chosen to avoid excessive leakage reactance, bearing in mind that the frequency of the rotor current is relatively high in the BDFM compared to that of a cage rotor in an induction machine.

B. Rotor windings

Employing two separate standard windings on the rotor, one for each pole number field is the simplest concept to understand but other designs which make better use of copper have been devised, starting with the work of Hunt [22] and more recently Oraee et al. [23]. The nested loop type of rotor [24] has been used in recent BDFMs. Whilst it was conceived as sharing the same simple construction as a normal cage rotor, Williamson et al. [25] showed that the bars needed to be insulated to constrain currents to particular paths, therefore acquiring the characteristic of a winding . This type of winding at its simplest comprises a number of loops equalling the sum of the pole-pair numbers of the BDFM, these loops being evenly spaced around the rotor circumference. This was described in [24] as a $p_1 + p_2$ phase system but as diametrically opposite loops have currents 180^o out of phase, it is actually a bi-$(p_1 + p_2)/2$ phase system. The turns ratio of the winding between the p_1 and p_2 sides is the ratio of the pitch factors, which are:

$$k_{p_1} = \sin\left(\frac{\gamma p_1}{2}\right) \tag{23}$$

$$k_{p_2} = \sin\left(\frac{\gamma p_2}{2}\right) \tag{24}$$

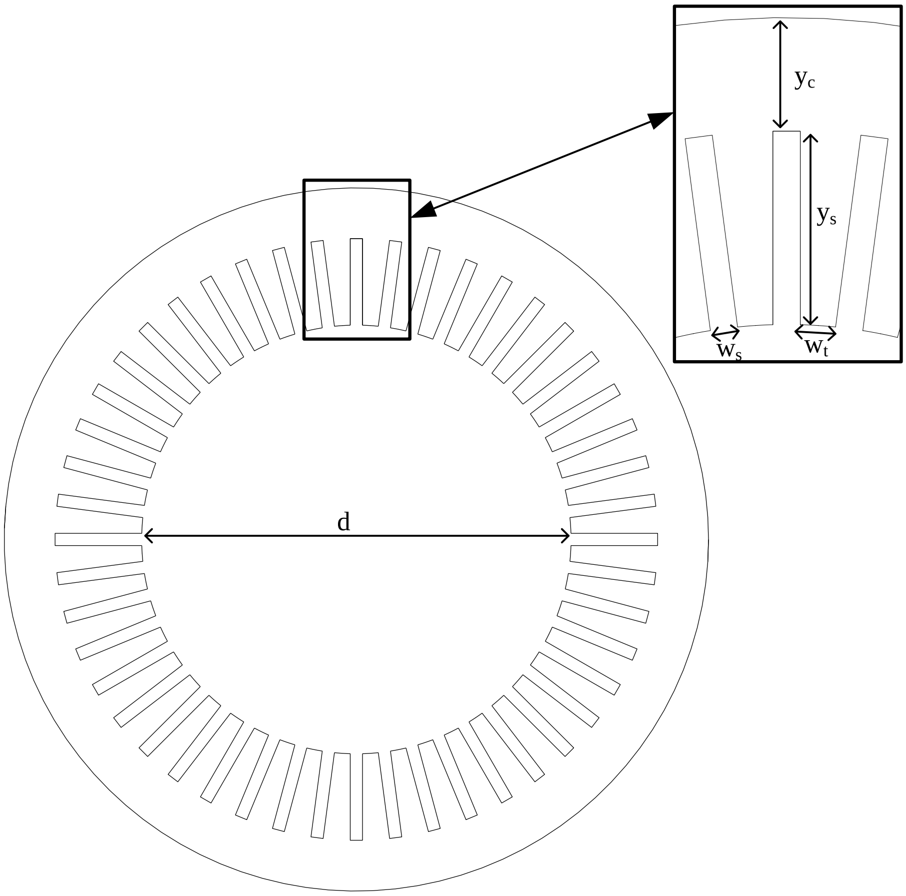

Fig. 4: Stator lamination showing key symbols

where γ is the pitch angle of the loop. For a 4/8 BDFM with a six bar cage, with loop spans of 60 degrees, this gives $k_{p1} = k_{p_2} = 0.87$, giving a turns ratio of unity. Alternatively the pitch of the six loops can be adjusted to give the optimum turns ratio according to Equations (8) or (9). One of the drawbacks of using single loops is the high space harmonic content and hence high rotor leakage inductance. Against this, large single conductors can be used,with a correspondingly high slot fill factor, provided that their dimensions do not approach those at which the skin effect becomes an issue.

Using multiple concentric loops to form nests, in the nested loop winding offers two advantages, the rotor will have a more even distribution of copper and there will be a reduction in space harmonics. However, the turns ratio for each loop will be different and so not only will loop currents differ but there will also be a degree of circulating currents. The uneven current distribution has implications for the electric loading but recent work [21] confirms that the rotor bars are thermally well coupled. The winding will exhibit an effective turns ratio, and this typically shows a small variation with the frequency of rotor currents. A method which gives reasonable results is given in [26].

In the nested loop type of rotor the same current distribution creates the p_1 and p_2 mmfs, and indeed the harmonic mmfs. The electric loading contributions can be expressed as:

$$\bar{J}_{r_{p1}} = \frac{2qk_{w1_r}N_{ph}I_r}{\pi d} \tag{25}$$

$$\bar{J}_{r_{p2}} = \frac{2qk_{w2_r}N_{ph}I_r}{\pi d} \tag{26}$$

Compared to rotors with separate p_1 and p_2 conventional poly-phase windings with winding factors close to unity, the total contribution for a given rotor conductor area and current density will be $k_{w1} + k_{w2}$ times as great, for example 1.57 times greater in the case of a 4/8 BDFM with a six loop rotor of optimum pitch. This gain can either be translated into a lower rotor resistance, a more compact rotor winding or used to compensate for the lower fill factor of multi-turn windings.

VIII. Validation of design formulae

The machine was originally constructed using the stator stack from a standard 4-pole induction machine which was then wound with 4-pole and 8-pole windings. The specially constructed rotor was a nested-loop rotor with 36 slots accommodating six nests each with three loops. The total electrical loading of the stator was 30.6 kA/m, with the power winding occupying 33 % of the stator slot area. However, the power winding was found to reach its electric loading limit before the control winding. In addition, although the stator was designed to work with a $B_{sum} = 0.86$ T, the rotor was not magnetically matched and saturation was evident above a B_{sum} of 0.46 T.

The stator of the machine was redesigned according equation (14) so that the power winding occupied 42 % of the slot area, enabling the two stator windings to reach their electrical loading limits simultaneously. A new nested-loop rotor was also built with increased tooth size to allow the machine to run at $B_{sum} = 0.96$ T. The physical dimensions of this BDFM together with stator and rotor winding details are given in Table II. A comparison of the original machine to the redesigned machine is shown in TableIII.

TABLE II: Physical parameters of a frame size 180 BDFM

Parameter	**Value**
Physical Dimensions	
Stack length	190 mm
Airgap diameter	175 mm
Airgap length with Carter factors	0.579 mm
Stator core back radial depth	20.7 mm
Stator tooth width	6.3 mm
Rotor core back radial depth	34.0 mm
Rotor tooth width	8.3 mm
Stator slot cross sectional area	135.5 mm^2
Rotor slot cross sectional area	95.7 mm^2
Stator slots	48
Rotor slots	36
Winding details	
Stator 1 poles	4
Stator 1 turns	160/phase 1.2 mm diameter wire
Stator 2 poles	8
Stator 2 turns	320/phase 1.2 mm diameter wire
Rotor type	nested-loop
Number of rotor slots/nests/loops	36/6/3
Rotor loop spans	10, 30, 50 degrees
Output	
Stator 1 rated current	7 A
Stator 2 rated current	7 A
Rated torque	112 Nm
Rotor turns ratio	
Computed	0.688
Extracted	0.685

Time stepping finite element analysis (TSFEA) simulations and corresponding experiments were performed for the operating conditions in Table V with the aim of verifying the design formulae of sections IV, V, and VI. Results from the TSFEA simulations were used to compute the peak airgap flux densities of the 4 and 8 pole fields together with the peak flux densities in the teeth and core back of the rotor and stator. These are given together with peak flux density values computed using equations (20) and (21), but with the same airgap flux densities calculated using TSFEA. The peak core back flux densities of both the stator and rotor compare well with a maximum error of 6.7%, for the stator core back values of the full load operation. The errors in peak flux density values in the teeth are larger for both the rotor and the stator but are within 10%. The main source of error between the predicted and modelled values is saturation, which is most severe in the teeth where the flux density is highest, as illustrated in Figures 5 and 6.

The magnetisation characteristics were determined with both stator windings excited and are shown in Figure 7. The BDFM was driven by an external machine at 750 rev/min with no load torque. The values of B_1 and B_2 were computed using terminal voltages accounting for stator voltage drops. B_{sum} was obtained from $B_1 + B_2$. Each data point was recorded for a balanced excitation condition, with each winding providing its own magnetizing current. This condition was achieved by adjusting the control winding voltage to minimize the rotor currents, for a given power winding voltage. At the full load operating conditions given in Table V with B_{sum} of 0.77 T (equivalent to a B_{quad} of 0.5 T), the onset of saturation is evident as shown in Figure 7.

TABLE III: Comparison between original and redesigned D180 BDFM

	Parameter	Original	Redesigned	Units
Stator	α	0.33	0.42	
	Electrical loading:			
	J_1	10.6	13.3	kA/m
	J_2	20.0	19.0	kA/m
	$\bar{J}$	30.6	32.3	kA/m
	Magnetic loading:			
	B_1	0.17	0.40	T
	B_2	0.29	0.56	T
	B_{sum}	0.46	0.96	T
	Slot area	135.5	135.5	mm^2
Rotor	Slot area	147.2	95.7	mm^2
	Tooth/slot dimensions:			
	y_s	19.5	23.0	mm
	w_s	9.4	6.7	mm
	w_t	5.7	8.3	mm
	Current density	3.4	5.4	A/mm^2
General	Torque	52	97	Nm
	Output power	3.13	6.3	kW
	Efficiency	0.77	0.82	

TABLE IV: Reduced equivalent circuit parameters for D180 BDFM

Parameter	**Value**
R_1	2.42 Ω
R_2	4.04 Ω
L_{m1}	457 mH
L_{m2}	493 mH
$R_r^{'}$	1.60 Ω
$L_r^{'}$	54 mH

Table VII shows a comparison of B_1 and B_2 values at no load and full load operating conditions. The values calculated from experimental measurements are close to the results computed using TSFEA.

The output powers from stator windings 1 and 2 were measured for the full load operating condition and are:

$$P_{c1} = 4025 \text{ W} \tag{27}$$

$$P_{c2} = 2241 \text{ W} \tag{28}$$

These are in the ratio

$$\frac{P_1}{P_2} = 0.557 \tag{29}$$

This is comparable, within a 10% error, to the ratio predicted using equation (10), which is 0.5. Therefore, equation (10) can be used for generating initial power estimates.

TABLE V: Operation and extraction conditions for the evaluation of design equations

Condition	**Torque (Nm)**	**V_1 (V)**	**V_2 (V)**	**Speed (rev/min)**
No load	0	240	176	750
Full load	-97	240	172	750

TABLE VI: Predicted flux densities in different parts of the machine compared with FE values

Torque (Nm)	B_1^{FE} (T)	B_2^{FE} (T)	$B_{t,s}$ (T)	$B_{t,s}^{FE}$ (T)	$B_{c,s}$ (T)	$B_{c,s}^{FE}$ (T)	$B_{t,r}$ (T)	$B_{t,r}^{FE}$ (T)	$B_{c,r}$ (T)	$B_{c,r}^{FE}$ (T)
0	0.30	0.41	1.82	1.73	1.50	1.46	1.84	1.67	0.91	0.92
-97	0.32	0.43	1.93	1.81	1.59	1.49	1.95	1.80	0.97	0.95

TABLE VII: Airgap flux density (RMS) values derived from terminal voltages compared to values computed using TSFEA

Torque (Nm)	B_1 (T)	B_1^{FE} (T)	B_2 (T)	B_2^{FE} (T)
0	0.30	0.30	0.42	0.41
-97	0.31	0.32	0.46	0.43

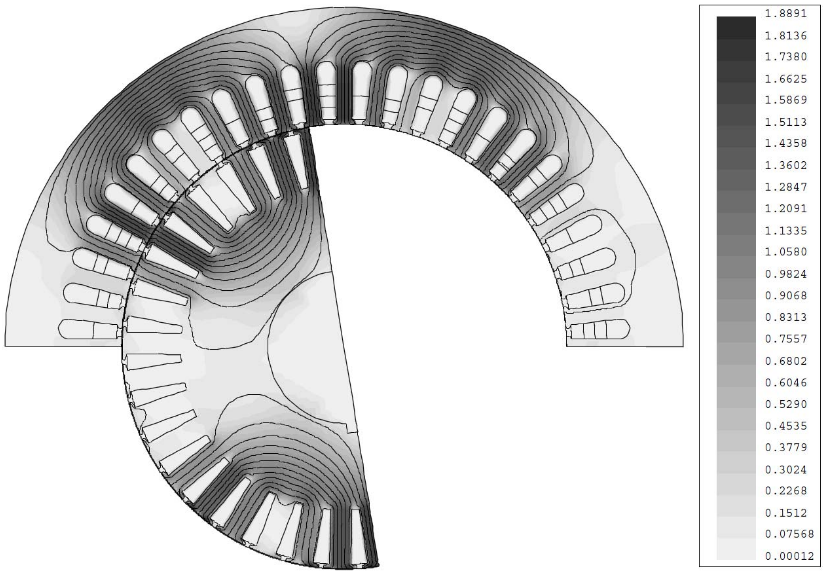

Fig. 5: Flux plot for operating condition with torque = 0 Nm

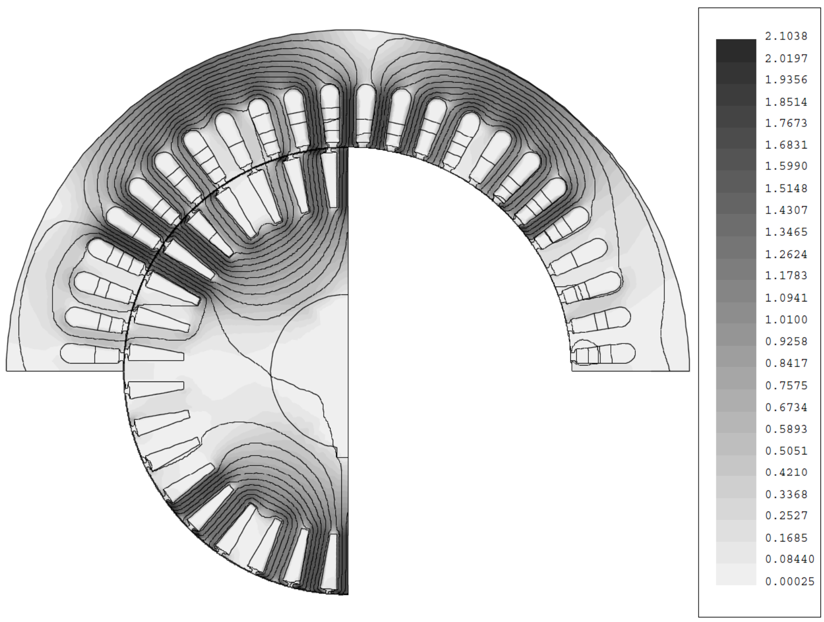

Fig. 6: Flux plot for operating condition with torque = -97 Nm

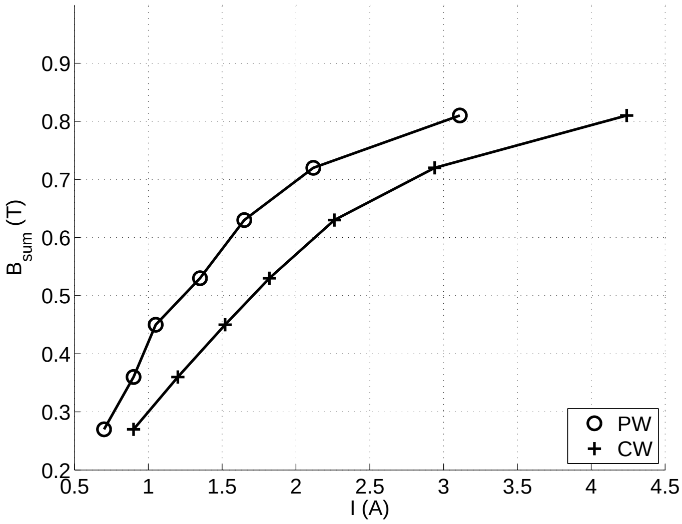

Fig. 7: B_{sum} values as a function of the power (PW) and control (CW) winding currents

TABLE VIII: B_{sum} values for magnetization test

V_1(V)	V_2(V)	B_1(T)	B_2(T)	B_{sum}(T)	B_{quad}(T)
90	66	0.11	0.16	0.27	0.19
120	87	0.15	0.21	0.36	0.26
150	108	0.19	0.26	0.45	0.32
180	130	0.22	0.31	0.53	0.38
210	152	0.26	0.37	0.63	0.45
240	176	0.30	0.42	0.72	0.52
270	205	0.33	0.48	0.81	0.58

IX. Conclusions

This paper outlines a design procedure for the BDFM which starts with the choice of pole-pair numbers to set the speed. Normal balanced three-phase windings are used for the stator windings, and these can be short-pitched. The rotor should have a turns ratio near optimum and the winding must be insulated to give determinate current paths. Equations are derived from the machines equivalent circuit to give an initial design. This can be refined by an iterative procedure which keeps the machine within electric and magnetic loading limits over a specified operating range. The approach is illustrated with results from a frame size 180 BDFM and the authors have also used the procedure to design a 250 kW BDFM [27]. The need to verify the magnetic circuit design by TSFEA is important and other methods are needed for a detailed assessment of harmonic effects and losses.

Appendix A

Optimum division of slot area

The optimum division of slot area between the stator windings is determined using minimum stator conduction losses as a criterion. The resistance per phase of stator winding 1 (R_1) is given by:

$$R_1 = \rho l_1 \frac{N_1}{A_{c1}} \tag{30}$$

Where l_1 is average length of a turn, ρ the resistivity, N_1 the number of turns, and A_{c1} is conductor cross-sectional area. The total cross-sectional area of the winding conductors (A_1) is given by:

$$A_1 = 2N_1 q A_{c1} \tag{31}$$

Where q is the number of phases. The conduction losses in this winding (P_1) are given by

$$P_1 = \frac{2q^2 \rho l_1 N_1^2 I_1^2}{A_1} \tag{32}$$

Where I_1 is the current. Similarly, the conduction losses of stator winding 2 (P_2) are given by:

$$P_2 = \frac{2q^2 \rho l_2 N_2^2 I_2^2}{A_2} \tag{33}$$

The parameters in equation (33) have similar meaning to those of equation (32). It is assumed that the average turn lengths are similar. I_2 is related to I_1 by [14]:

$$I_2 = \frac{I_1 N_1}{n_r N_2} \tag{34}$$

Therefore, the total stator conduction loss (P_o), which is equal to the sum of the conduction losses of stator windings 1 and 2, is given by:

$$P_o = 2q^2 \rho l_1 N_1^2 I_1^2 \left(\frac{1}{A_1} + \frac{1}{n_r^2 A_2} \right) \tag{35}$$

Let A_o be the total slot area occupied by the conductors of the stator windings. Additionally, let α, be a proportion of A_o, that is occupied by the conductors of stator 1 winding, such that:

$$A_1 = \alpha A_o \tag{36}$$

Therefore,

$$A_2 = (1 - \alpha) A_o \tag{37}$$

and equation (35) becomes:

$$P_o = 2q^2 \rho l_1 N_1^2 I_1^2 \left(\frac{1}{\alpha A_o} + \frac{1}{(1-\alpha)\, n_r^2 A_o} \right) \tag{38}$$

The minimum value of P_o is obtained for:

$$\alpha = \frac{n_r}{n_r + 1} \tag{39}$$

Appendix B

Derivation of BDFM output power from a 2 machine viewpoint

The power converted from the i^{th} stator winding (ignoring losses) is given as:

$$P_{c_i} = T_i \omega_r \tag{40}$$

With the output torque produced by the i^{th} stator winding given by:

$$T_i = \frac{\pi^2}{\sqrt{2}} \left(\frac{d}{2} \right)^2 l \bar{B}_i \bar{J}_i \tag{41}$$

The specific magnetic ($\bar{B}$) and electrical ($\bar{J}$) loading of each winding can be combined such that:

$$\bar{J} = \bar{J}_1 + \bar{J}_2 \qquad \bar{B} = \bar{B}_1 + \bar{B}_2 \tag{42}$$

This leads to a output power equation which is based on the sum of the power produced by the two stator windings.

$$P_c = \frac{\pi^2}{\sqrt{2}} \left(\frac{d}{2} \right)^2 l \omega_r \left(\bar{B}_1 \bar{J}_1 + \bar{B}_2 \bar{J}_2 \right) \tag{43}$$

The specific electrical ($\bar{J}$) of each winding is given by:

$$\bar{J}_1 = \bar{J}\left(\frac{1}{1+\frac{1}{n_r}}\right) \tag{44}$$

$$\bar{J}_2 = \bar{J}\left(\frac{1}{1+n_r}\right) \tag{45}$$

The specific magnetic ($\bar{B}$) of each winding is determined by solving (5) and (16) simultaneously:

$$\bar{B}_1 = \frac{\bar{B}}{\left(1+\frac{p_2 n_r}{p_1}\frac{\cos\phi}{\cos(\phi+\delta)}\right)} \tag{46}$$

$$\bar{B}_2 = \frac{\bar{B}}{\left(1+\frac{p_1}{p_2 n_r}\frac{\cos(\phi+\delta)}{\cos\phi}\right)} \tag{47}$$

Substituting (44) - (47) into (43) yields:

$$P_c = \frac{\pi^2}{\sqrt{2}}\left(\frac{d}{2}\right)^2 l\omega_r \bar{B}\bar{J}_c\left(\frac{p_1 + p_2\left(\frac{\cos\phi}{\cos(\phi+\delta)}\right)}{p_1\left(1+\frac{1}{n_r}\right)\left(1+\frac{p_2 n_r}{p_1}\frac{\cos\phi}{\cos(\phi+\delta)}\right)}\right) \tag{48}$$

APPENDIX C
CASE STUDY: INITIAL DESIGN OF 250 KW BDFM

The following section presents the process of establishing an initial design for the 250 kW BDFM [28] based on the equations presented in this paper. The design uses the optimum turns ratio (not the actual one) and space harmonics [26] are ignored. The stator windings are not short pitched and magnetizing currents are ignored. Once an initial design has been made, an iterative process can begin, where the actual turns ratio is used, and magnetizing currents are included.

A. Inputs

Pole pairs: $p_1 = 2$, $p_2 = 4$ (chosen for synchronous speed of 500 rev/min)

Phases: $q = 3$

Supply voltage: $v_1 = 690$ V, $v_2 = 620$ V

Supply Frequency: $f_1 = 50$ Hz, $f_2 = \pm 18$ Hz

Specific electrical loading: $\bar{J}_c = 46$ kA/m (suggested by machine manufacturer)

Current density: $J_s = 3.5$ A/mm^2 (suggested by machine manufacturer)

Stator fill factor: $c_p = 0.6$ (suggested by machine manufacturer)

Airgap diameter: $d = 0.439$ m (based on an initial D400 frame size, and to target the specific output power based on (48))

Stack length: $l = 0.732$ m (based on an initial D400 frame size, and to target the specific output power based on (48))

Air gap: $g = 1$ mm (as small as mechanically possible)

Stator slots: $n_s = 72$ (appropriate for a machine of this size)

Stator flux density: B_{sum} = 0.7 T

Peak flux density: $\hat{B}_t = 1.8$ T, $\hat{B}_c = 1.6$ T (past experience and through FEA)

B. Outputs

Specific magnetic loading: $\bar{B} = \frac{2\sqrt{2}}{\pi} B_{sum} = 0.630$ T

Optimum turns ratio: $n_r = \left(\frac{p_1}{p_2}\right)^{\frac{1}{2}} = \left(\frac{2}{4}\right)^{\frac{1}{2}} = 0.707$

Rated rotational speed: $\omega_r = \frac{\omega_1+\omega_2}{p_1+p_2} = \frac{2\pi f_1+2\pi f_2}{p_1+p_2} = 71.2$ rad/s

Output power (unity power factor): $P_c = \frac{\pi^2}{\sqrt{2}}\left(\frac{d}{2}\right)^2 l\omega_r \bar{B}\bar{J}_c \left(\frac{p_1+p_2}{p_1\left(1+\frac{1}{n_r}\right)\left(1+n_r\frac{p_2}{p_1}\right)}\right) = 262$ kW

Airgap magnetic field for each stator winding: $B_1 = B_{sum}\frac{p_1}{p_1+n_r p_2} = 0.29$ T, $B_2 = B_{sum} - B_1 = 0.41$ T

Slot pitch: $\beta = \frac{2\pi}{n_s} = \frac{2\pi}{72}$

Winding Factor (no short pitching): $k_w = \frac{\sin\left(\frac{n_s\beta}{4q}\right)}{\frac{n_s}{2qp}\sin\left(\frac{\beta p}{2}\right)}$, $k_{w1} = 0.956$, $k_{w2} = 0.960$

Stator turns: $N_1 = \frac{p_1 v_1}{2\pi f_1 l d k_{w1} B_1} = 49.3$, $N_2 = \frac{p_2 v_2}{2\pi f_2 l d k_{w2} B_2} = 173.4$

Actual turns (closest allowable integer): $N_1 = 48$, $N_2 = 168$

Stator tooth width: $w_t = \frac{\sqrt{2}\pi d}{n_s \hat{B}_t}\left(B_1 + B_2\right) = 10.5$ mm

Stator slot width: $w_s = \frac{\pi(d+g) - n_s w_t}{n_s} = 8.7$ mm

Stator core back depth: $y_c = \frac{\sqrt{2}d}{2\hat{B}_c}\left(\frac{B_1}{p_1} + \frac{B_2}{p_2}\right) = 48$ mm

Slot depth: $y_s = \frac{\bar{J}_c}{J_s c_p\left(1-\frac{\bar{B}\pi}{2\hat{B}_t}\right)} = 48.7$ mm

Stator slot area: $A_s = w_s y_s = 421.7$ mm^2 (assuming parallel slots, tapered teeth)

Proportion of slot area assigned to stator 1: $\alpha = \frac{1}{1+\frac{1}{n_r}} = 0.414$

Total cross-sectional area of each winding: $A_1 = \alpha c_p A_s n_s = 7546$ mm^2, $A_2 = (1-\alpha)c_p A_s n_s = 10672$ mm^2

Conductor cross-sectional area: $A_{c1} = \frac{A_1}{2N_1 q} = 26.2$ mm^2, $A_{c2} = \frac{A_2}{2N_2 q} = 10.6$ mm^2

Phase current: $I_1 = J_s A_{c1} = 91.7$ A, $I_2 = J_s A_{c2} = 37.1$ A

Conduction losses: $P_{1,2} = \frac{2q^2\rho l N_{1,2}^2 I_{1,2}^2}{A_{1,2}}$, $P_1 = 1.8$ kW, $P_2 = 2.0$ kW

REFERENCES

[1] A. Wallace, R. Spée, and G. C. Alexander, "Adjustable speed drive and variable speed generation systems with reduced power converter requirements," in *Conference Proceedings, ISIE'93, IEEE international Symposium on Industrial Electronics*. IEEE, 1-3 June 1993, pp. 503–508, budapest.

[2] C. S. Brune, R. Spée, and A. K. Wallace, "Experimental evaluation of a variable-speed, doubly-fed wind-power generation system," *IEEE Trans. Industry Applications*, vol. 30, no. 3, pp. 648–655, May/June 1994.

[3] R. A. McMahon, X. Wang, E. Abdi-Jalebi, P. Tavner, P. C. Roberts, and M. Jagiela, "The bdfm as a generator in wind turbines," in *Power Electronics and Motion Control Conference, 2006. EPE-PEMC 2006. 12th International*, Aug 2006, pp. 1859–1865.

[4] H. Arabian-Hoseynabadia, H. Oraee, and P. Tavner, "Failure modes and effect analysis (fmea), wind turbines, brushless doubly fed generator (bdfg)," *International journal of electrical power and energy systems*, vol. 32, pp. 817–824, 2010.

[5] S. Shao, E. Abdi, and R. McMahon, "Operation of brushless doubly-fed machine for drive applications," in *Power Electronics, Machines and Drives, 2008. PEMD 2008. 4th IET Conference on*, April 2008, pp. 340–344.

[6] A. R. W. Broadway and L. Burbridge, "Self-cascaded machine: a low-speed motor or high frequency brushless alternator," *Proceedings, Institution of Electrical Engineers*, vol. 117, pp. 1277–1290, 1970.

[7] P. Rochelle, R. Spée, and A. K. Wallace, "The effect of stator winding configuration on the performance of brushless doubly-fed machines in adjustable speed drives," in *Conference record of the IEEE Industry Applications Society Annual Meeting*. Seattle,WA: IEEE, October 7-12 1990, pp. 331–337.

[8] T. Logan, J. Warrington, S. Shao, and R. McMahon, "Practical deployment of the brushless doubly-fed machine in a medium scale wind turbine," in *Power Electronics and Drive Systems, 2009. PEDS 2009. International Conference on*, Nov 2009, pp. 470–475.

[9] S. Williamson and A. C. Ferreira, "Generalised theory of the brushless doubly-fed machine. Part 2: model verification and performance," *IEE Proceedings - Electric Power Applications*, vol. 144, no. 2, pp. 123–129, 1997.

[10] P. C. Roberts, R. A. McMahon, P. J. Tavner, J. M. Maciejowski, and T. J. Flack, "Equivalent circuit for the brushless doubly-fed machine (BDFM) including parameter estimation," *Proc. IEE B - Elec. Power App.*, vol. 152, no. 4, pp. 933–942, July 2005.
[11] Y. Liao, "Design of a brushless doubly-fed induction motor for adjustable speed drive applications," in *Proc. IEEE Industry App. Soc. Annual Mtg.* IEEE, 6-10 October 1996, pp. 850–855.
[12] X. Wang, R. McMahon, and P. Tavner, "Design of the brushless doubly-fed (induction) machine," in *Electric Machines Drives Conference, 2007. IEMDC '07. IEEE International*, vol. 2, May 2007, pp. 1508–1513.
[13] F. Rüncos, R. Carlson, N. Sadowski, P. Kuo-Peng, and H. Voltolini, "Performance and vibration analysis of a 75 kw brushless double-fed induction generator prototype," in *Industry Applications Conference, 2006. 41st IAS Annual Meeting. Conference Record of the 2006 IEEE*, vol. 5, Oct 2006, pp. 2395–2402.
[14] R. A. McMahon, P. C. Roberts, X. Wang, and P. J. Tavner, "Performance of the BDFM as a generator and a motor," *Proc. IEE B - Elec. Power App.*, March 2006.
[15] S. Williamson, A. C. Ferreira, and A. K. Wallace, "Generalised theory of the brushless doubly-fed machine. Part 1: Analysis," *IEE Proceedings - Electric Power Applications*, vol. 144, no. 2, pp. 111–122, 1997.
[16] F. Creedy, "Some developments in multi-speed cascade induction motors," *Institution of Electrical Engineers, Journal*, pp. 511–537, 1920.
[17] T. Logan, R. McMahon, and K. Seffen, "Noise and vibration in brushless doubly fed machine and brushless doubly fed reluctance machine," *Electric Power Applications, IET*, vol. 8, no. 2, pp. 50–59, February 2014.
[18] F. Rüncos, R. Carlson, A. M. Oliveira, P. Kuo-Peng, and N. Sadowski, "Performance analysis of a brushless doubly-fed cage induction generator," in *Proc. 2nd Nordic Windpower Conf.*, 2004, 1-2 March.
[19] A. C. Ferreira and S. Williamson, "Time-stepping finite-element analysis of brushless doubly fed machine taking iron loss and saturation into account," *IEEE Transactions on Industry Applications*, vol. 35, no. 3, pp. 583–588, 1999.
[20] S. Abdi, E. Abdi, and R. McMahon, "Optimisation of magnetic circuit for brushless doubly fed machines," *IEEE Transactions on Energy Conversion*, vol. Accepted for publication, 2015.
[21] M. Mathekga, R. McMahon, S. Shao, and D. Staton, "Study of the electric loading aspects of the bdfm using a lumped parameter thermal model," in *Power Electronics, Machines and Drives (PEMD 2010), 5th IET International Conference on*, April 2010, pp. 1–6.
[22] L. J. Hunt, "A new type of induction motor," *Institution of Electrical Engineers, Journal*, pp. 648–677, 1907.
[23] A. Oraee, E. Abdi, S. Abdi, R. McMahon, and P. Tavner, "Effects of rotor winding structure on the bdfm equivalent circuit parameters," *Energy Conversion, IEEE Transactions on*, vol. PP, no. 99, pp. 1–10, 2015.
[24] A. R. W. Broadway, "Brushless cascade alternator," *Proc. IEE*, vol. 121, no. 12, pp. 1529–1535, 1974.
[25] S. Williamson and M. Boger, "Impact of inter-bar current on the performance of the brushless doubly fed motor," *IEEE Trans. Industry Applications*, vol. 35, no. 2, pp. 453–460, March/April 1999.
[26] R. McMahon, P. Roberts, M. Tatlow, E. Abdi, A. Broekhof, and S. Abdi, "Rotor parameter determination for the brushless doubly fed (induction) machine," *Electric Power Applications, IET*, vol. 9, no. 8, pp. 549–555, 2015.
[27] R. McMahon, E. Abdi, P. Malliband, S. Shao, M. E. Mathekga, and P. Tavner, "Design and testing of a 250 kw medium-speed brushless dfig," in *Power Electronics, Machines and Drives (PEMD 2012), 6th IET International Conference on*, March 2012, pp. 1–6.
[28] E. Abdi, R. McMahon, P. Malliband, S. Shao, E. Mathekga, P. Tavner, S. Abdi, A. Oraee, T. Long, and M. Tatlow, "Performance analysis and testing of a 250 kw medium-speed brushless doubly-fed induction generator," *Renewable Power Generation, IET*, vol. 7, pp. 631 – 638, 2013.